iScience

CellPress
OPEN ACCESS

Article

5G and energy internet planning for power and communication network expansion

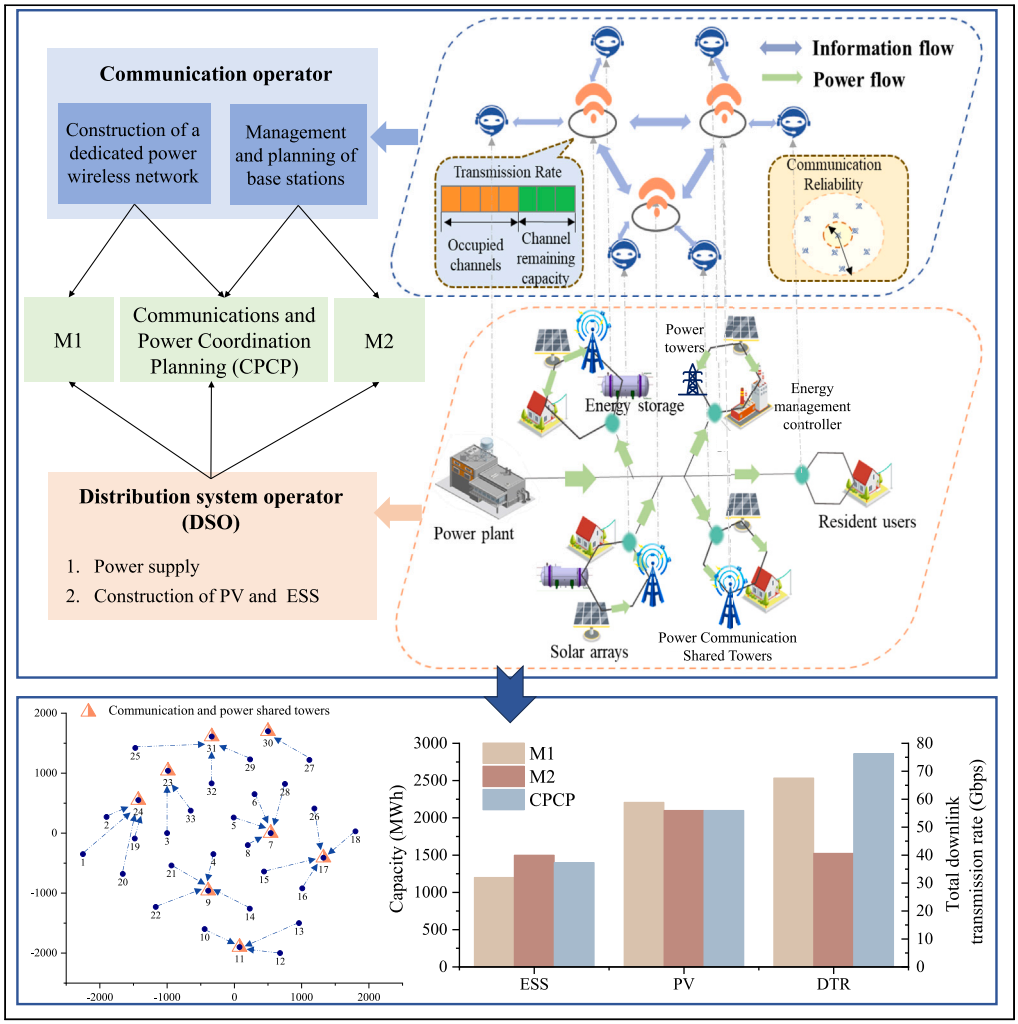

Lin Chen, Jianxiao Wang, Zhaoyuan Wu, Yang Yu, Ming Zhou, Gengyin Li

wang-jx@pku.edu.cn

Highlights

Strategic base station placement reduces energy disruption risk

CPCP enhances reliability and speed in communication

CPCP reduces costs and supports green energy

Study emphasizes planning for resilient energy futures

Chen et al., iScience *27*, 109290
March 15, 2024
https://doi.org/10.1016/j.isci.2024.109290

iScience

CellPress
OPEN ACCESS

Article

5G and energy internet planning for power and communication network expansion

Lin Chen,[1] Jianxiao Wang,[2,3,5,*] Zhaoyuan Wu,[4] Yang Yu,[1] Ming Zhou,[4] and Gengyin Li[4]

SUMMARY

Our research addresses the critical intersection of communication and power systems in the era of advanced information technologies. We highlight the strategic importance of communication base station placement, as its optimization is vital for minimizing operational disruptions in energy systems. Our study introduces a communications and power coordination planning (CPCP) model that encompasses both distributed energy resources and base stations to improve communication quality of service. This model facilitates optimal resource distribution, ensuring communication reliability over 96% and downlink transmission rates above 450 Mbps, enhancing network resilience and cost-effectiveness. Through case studies, we demonstrate CPCP's potential to significantly reduce planning costs, particularly with increased renewable energy integration, supporting the transition to low-carbon energy systems. Our findings contribute to a comprehensive understanding of the symbiotic relationship between communication and power networks, emphasizing the need for coordinated planning in building future-proof energy infrastructures.

INTRODUCTION

The development of information and communications technology, as well as distributed energy resources (DERs), has become an important means of achieving an efficient and clean energy system.[1] As the number of available DERs increases, this will have an enormous impact on future power system architecture.[2] The most typical change is the emergence of a large number of regional autonomous microgrids (MGs), which can actively control power flow and interact with loads. With access to massive-scale DERs and the application of intelligent measurement equipment, the secure, reliable, and efficient operation of power systems requires the support of advanced information and communication technology (ICT).[3–5] In the communication field, recent years have witnessed the rapid development of various communication-related technologies, including standards formulation and base station (BS) construction, which have advanced in leaps and bounds.[6] Compared to 4G, 5G communication has much higher performance in terms of transmission rate, time delay, and other indicators. China has deployed 690,000 5G BSs, and the number of terminal connections exceeds 180 million. It is estimated that by 2030, the number of 5G BSs operating in China will exceed 10 million.[7] With the construction of such a massive number of 5G BSs, on the one hand, the energy consumption of communication systems will present new challenges and problems for the energy management of power systems.[8] On the other hand, the existing number of towers for communication operators is not enough to support large-scale BS construction, and a large number of new towers are not only a huge investment, but also a waste of land resources.

To this end, Distribution System Operators (DSOs) and communication operators sought a new mode of cooperation, and shared towers were born.[9] The development of the power system has so far formed a more complete transmission and distribution network, with abundant pole and tower resources, and the power poles spread all over the place provide a good opportunity for sharing towers. The shared tower is a new resource-sharing model in which a communication BS is added to a power tower, allowing the power line and BS to share a tower. Therefore, power systems and communication systems are increasingly coupled. A power system supplies energy, and a communication system meets the demand for information exchange. A BS is the main intermediary between a communication network and a power network. For the communication network, it is an important transfer point for wireless information transmission. For the power network, it is the main communication device and consumes electricity.[8] With the continuous coupling of communication and power systems, it is necessary to comprehensively plan the capacities and geographic locations of BSs by integrating the power loads, the communication loads and the situation regarding new-energy-based power generation so as to realize the coordinated planning of the 5G communication system infrastructure and the distribution network.[10]

The planning of ADNs has been extensively addressed in the studies over the past decades, which mainly focuses on the optimal planning of various elements in the distribution network (i.e., DERs, circuit breakers, energy storage, and capacitors[11–14]) to ensure the security and

[1]Institute for Interdisciplinary Information Sciences, Tsinghua University, Beijing 100084, China
[2]National Engineering Laboratory for Big Data Analysis and Applications, Peking University, Beijing 100871, China
[3]Peking University Ordos Research Institute of Energy, Ordos 017000, China
[4]School of Electrical and Electronic Engineering, North China Electric Power University, Beijing 102206, China
[5]Lead contact
*Correspondence: wang-jx@pku.edu.cn
https://doi.org/10.1016/j.isci.2024.109290

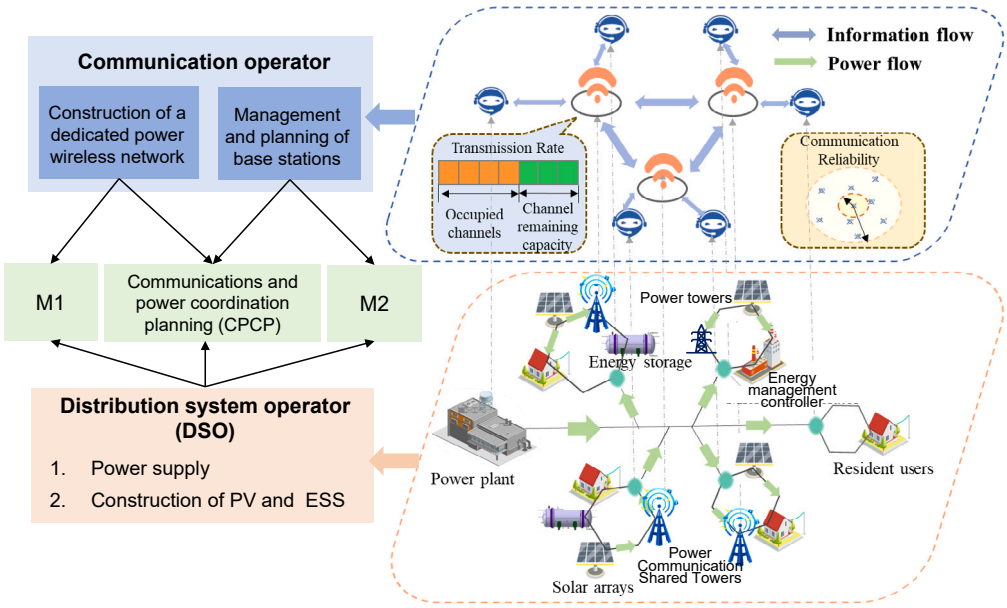

Figure 1. The framework of the cooperation strategies

reliability of distribution system operation. With the deepening of the coupling degree between communication and power systems, studies have also emerged on planning methods for communication resources (i.e., signal processing devices, BS power supply devices, and the spectrum of communication networks[15–17]). In the study by Mao et al.[18] the incurred cost of BSs in the communication network is taken into account. Even though, the aforementioned literature provides useful insights into the coordinated operation of both the energy and the communication system. Nevertheless, these studies only optimized and scheduled the power resources and communication resources of BSs from the perspective of the communication system, without considering the impact of the topological location of the BS on the power system.

In practice, with the further construction of 5G communication system, the density of 5G BSs will increase significantly, and the corresponding energy consumption of the communication system can no longer be neglected.[19] The coupling between the energy and communication systems is convinced to be strengthened.[20] On the one hand, the operation strategy of the communication system may change the original power flows of the distribution networks. On the other hand, the reliable coordinated operation depends on the efficient support of the communication system. Therefore, the coordinated planning of communication resources and power resources taking into account the power topology can improve the communication quality while ensuring the efficient operation of the energy system, which is worthy of further study.

In our previous work,[21] we introduced the modeling of communication reliability (CR) to capture the mutual impacts of cyber-physical systems, and proposed a CR-restricted coordinated operation strategy in active distribution networks. However, the coordinated planning of communication and energy systems is supposed to ensure sufficient CR and the different communication requirements of heterogeneous users, i.e., an access mechanism for the BSs. To fill the aforementioned gap, we introduce and explore a strategy, communications and power coordination planning (CPCP), which is dedicated to achieving efficient coordination between distributed energy systems and communication networks. To accomplish this objective, we first propose a BS access mechanism to determine an efficient communication topology among MGs and BSs. Subsequently, we develop a coordinated planning model that takes into consideration key communication quality indicators such as CR and downlink transmission rate. We employ a multiple linear regression model to incorporate these metrics into the coordinated planning model, providing better consideration of their nonlinear characteristics. Through case studies based on both standard and real-world distribution networks, we validate the effectiveness of the CPCP strategy, demonstrating its potential to enhance communication quality while accounting for the deployment of DERs and BSs. This research underscores the crucial role of efficient communication infrastructure in modern power systems and presents a comprehensive approach that can be used to plan and operate both communication and power systems, ultimately leading to more resilient, efficient, and reliable networks.

RESULTS AND DISCUSSION

Framework

Figure 1 illustrates the concept of cooperation between communication operators and DSOs at the energy layer and communication layer. As shown in Figure 1, we consider a city-level distribution power system consisting of multiple MGs with DERs as well as battery storage systems. The DSO transmits electricity to the MG via power towers. The MG is managed by an energy management controllers (EMCs) that coordinates

Table 1. The characteristics of the three cooperative strategies

Strategies	Management and planning right of BS	Power wireless network construction
M1	×	✓
M2	✓	×
Communications and Power Coordination Planning (CPCP)	✓	✓

the dispatch of energy in the MG by interacting with information from other EMCs. This information can be interacted with through a communication network. Therefore, BSs are the main intermediaries between communication and energy systems. For the communication network, a BS is an important transfer point for wireless information transmission. For the distribution network, it is the main communication device and consumes electricity. The communications operator is responsible for the construction of BSs. However, the communication operator builds the BS to complement the 5G signal, and the establishment of a communication BS does not mean the establishment of a dedicated power wireless network. EMC can also communicate by accessing a normal 5G network but at a reduced reliability and transmission rate. The cooperation strategy of the two operators determines the establishment of a dedicated communications network. In the communications cooperation strategy, the communications operator establishes a dedicated power wireless network and the DSO provides the power supply and establishes the supporting distributed photovoltaic (PV) and energy storage under this MG.

The planning and management of BSs involve the impact of signals at the communication level and the distribution of electricity flow at the power level. This right is therefore vested differently under different cooperation strategies. In the M2 strategy, the DSO is given the right to manage and plan the BSs, and the DSO coordinates the planning of distributed energy in the distribution network and the selection of shared towers for electricity and communications. However, in this strategy, the communications operator does not provide the construction of a dedicated network.

In order to provide a better service to the power system, we propose a cooperation strategy of joint planning and communication. Communication operators not only set up dedicated power wireless networks, but also handed over the management and planning of BSs to DSO. It needs to be understood that this cession of rights will necessarily cost the DSO more money. However, it is beyond the scope of this paper to discuss how to incentivize the formation of this strategy. In addition to CPCP, we set up two comparison scenarios, M1 and M2, as shown in Table 1.

In this study, we first validate the CPCP method using the IEEE 33-bus system as a standard benchmark. The IEEE 33-bus system consists of multiple MGs, with adjustable loads at each node, serving as potential locations for the deployment of PV panels, energy storage systems (ESSs), and BSs. The study incorporates key parameters, including discount rate, service lives, and investment costs, which are further detailed in the STAR Methods section for reference. Subsequently, we apply the CPCP strategy to a real-world scenario in Venezuela, specifically in a zone within the metropolitan area of Caracas.[22] The evaluation in this case remains consistent with the parameters established earlier based on the IEEE 33-bus system, ensuring a comprehensive comparison across the three coordination strategies. The load and solar power data of the MGs are collected from ref.[23]

Communications and power coordination planning

In CPCP, mobile network operators not only transfer the planning and management rights of BSs to the DSO but also establish a dedicated power wireless network for the DSO. In turn, the DSO constructs supporting power supply equipment to ensure an ample energy supply for the mobile network operators. CPCP offers a comprehensive solution that addresses multiple critical aspects. It seeks to optimize the utilization of resources and enhance network performance in a holistic manner. In stark contrast to the M1 and M2 strategies, CPCP demonstrates several key advantages.

At its core, CPCP takes a meticulous approach to resource allocation for power generation and storage, as shown in Table 2. We carefully consider the energy demands of the distribution power system, ensuring that construction capacities for PV panels and ESS are aligned with the network's energy requirements. Unlike M1, which often concentrates shared tower locations in central areas for convenience and accessibility, CPCP strategically distributes these resources, resulting in a more balanced allocation (Figure 2B). This approach significantly reduces potential disparities in power flow across the distribution network, thereby optimizing resource utilization. It intelligently allocates towers with high power consumption to different feeders, ensuring a more even distribution of energy demand as shown in Figure 2A. In contrast, M1 tends to overlook this critical aspect, potentially leading to imbalances in energy distribution.

Additionally, at the cyber layer, CPCP goes beyond power considerations to enhance CR and downlink transmission rates. By strategically placing BSs and optimizing their accessibility for EMCs, CPCP maximizes the quality of communication services (QoS). It even offers intelligent routing of EMCs to alternative nearby BSs when the nearest BS is at full capacity, accounting for BS limitations. The results in Figure 2C reinforce the rationality and effectiveness of CPCP strategy. We observe that the achieved CR surpasses 96%, with a significant proportion of EMCs achieving a flawless 100% reliability. Furthermore, the downlink transmission rates consistently exceed the threshold of 450 Mbps, with EMCs connected to BSs achieving even higher rates, reaching up to 800 Mbps. This improvement in communication performance is facilitated by the provision of a dedicated power wireless network. The total downlink transmission capacity of 18.15 Gbps demonstrates the efficiency and effectiveness of our proposed CPCP strategy in addressing the communication demands of the network.

Table 2. Investment costs and capacities for energy storage, photovoltaics and base stations in the IEEE 33-bus system under the Communications and Power Coordination Planning (CPCP) strategy

	ESS	PV	BS
Capacity/number (MW)	420	1091	8
Investment cost (10^6 $)	3.62	33.94	11.08

In stark contrast, the M2 strategy raises concerns when it comes to CR and performance. Under this strategy, the delegation of BS management to the DSO occurs without the provision of dedicated wireless network construction services for the distribution network. As observed in Figure 2D, several EMCs under the M2 strategy, including EMCs 3, 8, 11, 13, 15, 25, and 33, experience significantly lower CR values below the predefined threshold of 96%. This deficiency in communication quality may lead to information transmission failures during coordinated operations, potentially incurring additional operational costs due to unstable communication. Furthermore, a substantial number of EMCs in the M2 strategy experience downlink transmission rates below the threshold of 450 Mbps. This suboptimal performance can hinder real-time energy sharing instructions among EMCs and result in delays in control actions, compromising the efficiency of energy sharing and coordination among energy users.

In summary, CPCP presents a holistic approach that optimizes both the power and communication aspects of network planning. At the electrical level, CPCP ensures efficient resource allocation for power generation and distribution, reducing disparities in power flow and enhancing resource utilization. Simultaneously, at the communication level, CPCP leverages a dedicated power wireless network and intelligent routing, resulting in superior CR and downlink transmission rates.

An application of the communications and power coordination planning strategy to Venezuela

Figure 3 presents a comparative assessment of the planning results under these three strategies in a distribution network of Venezuela. Notably, the M2 strategy achieves the lowest planning cost in Figure 3A, primarily due to its omission of a dedicated power wireless network. This eliminates the need to increase the power load of BSs. However, it's essential to emphasize that the M2 strategy falls short in terms of downlink transmission rate (DTR) compared to CPCP. This underscores the critical role of a dedicated power wireless network in the overall planning process. CPCP, on the other hand, exhibits higher DTR compared to M1, thanks to its coordinated planning approach. This approach allows BSs to utilize surplus DER output, increasing their transmit power to mitigate line congestion and enhance overall communication rates.

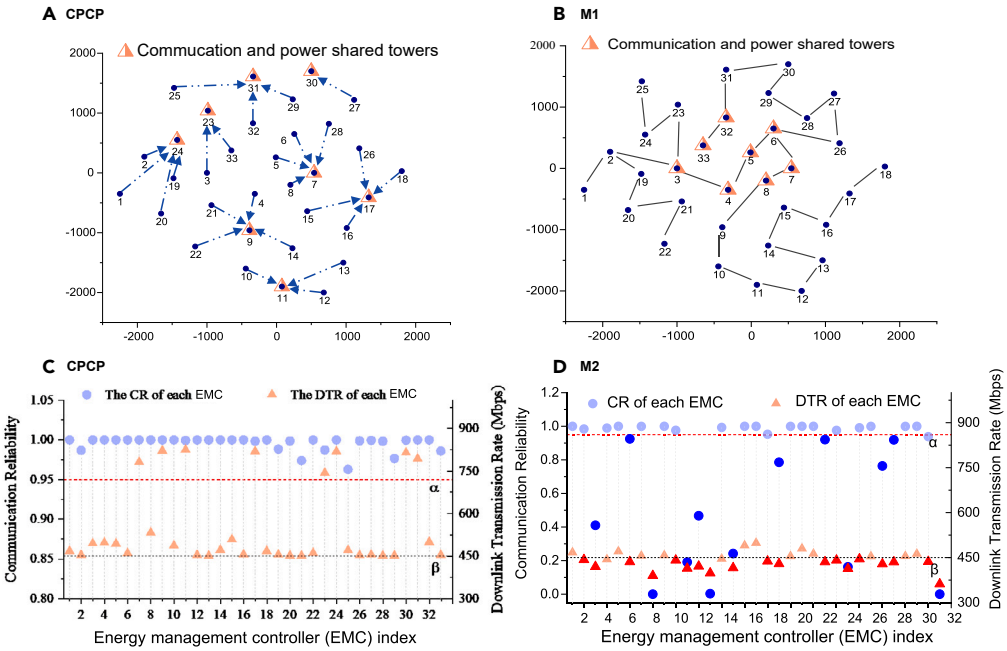

Figure 2. Comparison of planning results under communications and power coordination planning (CPCP) strategy, M1 and M2

(A) The selection of shared towers for power communications and the access of energy users represented by EMC under CPCP.

(B) The selection of communication power sharing base stations under M1.

(C) The communication reliability and downlink transmission rate under CPCP.

(D) The communication reliability and downlink transmission rate under M2.

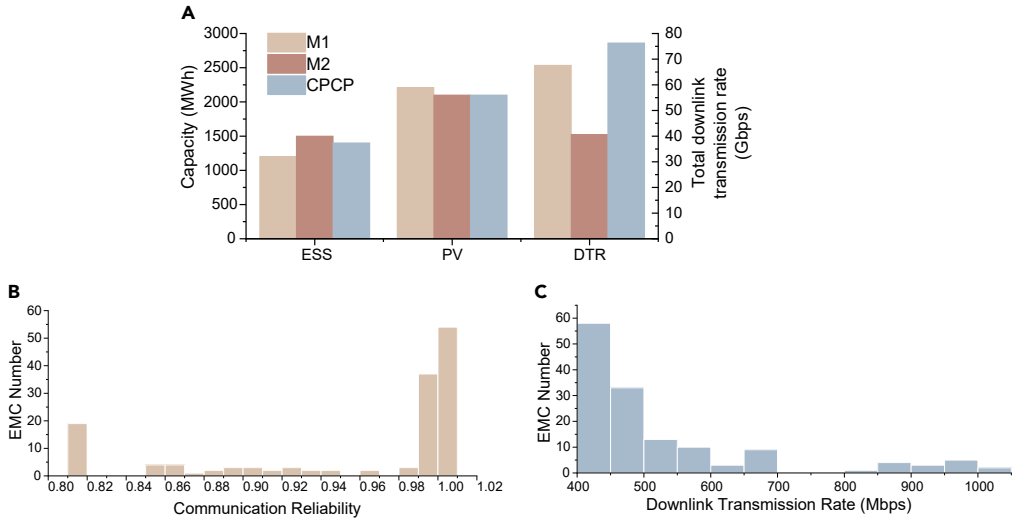

Figure 3. A comparative assessment of the planning results under three strategies in a distribution network of Venezuela

(A) The total investment capacity of energy storage and photovoltaics in the system, and the total downlink transmission rate of system users.

(B) Statistical graphs of the communication reliability under communications and power coordination planning (CPCP).

(C) Statistical graphs of the downlink transmission rate under CPCP.

Figures 3B and 3C provide insights into the communication quality statistics for the EMCs within the network. CPCP demonstrates its superiority in ensuring robust communication services, with approximately 64% of MGs achieving CR above 98%. Furthermore, the majority of EMCs experiences downlink transmission rates within the range of 400–550 Mbps. These results highlight the enhanced communication services accessible to all MGs through the adoption of the CPCP strategy.

In summary, the CPCP strategy emerges as a powerful solution for optimizing the joint coordination of power and communication systems within Venezuela's distribution network. It ensures the establishment of a dedicated power wireless network, resulting in robust and reliable communication infrastructure. This, in turn, facilitates fast and efficient data transmission, surpassing the CR requirement and the downlink transmission rate threshold. CPCP also strategically places BSs to maximize accessibility, optimizing QoS while minimizing interference. Additionally, CPCP enables coordinated planning between the distribution network and the communication network, enhancing overall communication rates by leveraging surplus DER output and addressing line congestion. These collective benefits demonstrate the CPCP strategy's effectiveness and efficiency in ensuring reliable and high-performance communication services within the network, contributing to improved user experiences and operational efficiency.

Coordinated planning of power and communication networks for enhanced low-carbon transition

As the challenges of future low-carbon transition intensify, the transformation of distribution networks, particularly toward zero-carbon MGs, becomes paramount. In this context, coordinated planning of power and communication networks emerges as a pivotal step in facilitating the low-carbon transition, offering substantial cost advantages. As illustrated in Figure 4A, the investment cost reduction achieved by the CPCP strategy, when compared to M1, increases from $1.5 million at a 20% renewable energy generation requirement to $1.8 million at a 100% renewable energy generation requirement. This shift in investment cost differential underscores the significance of coordinated planning. It not only enhances our ability to meet future energy demands efficiently but also lowers overall operational costs, contributing to a more sustainable and low-carbon energy network.

Furthermore, as depicted in Figure 4B, we observe changes in ESS and PV capacities, as well as total investment costs under the CPCP strategy, for different renewable energy generation ratios. It's important to note that only when the proportion of renewable energy sources surpasses the threshold of 60%, there is a sharp increase in investment costs. This phenomenon occurs because within the MGs, there is already an inherent PV energy output, allowing it to reach the output ratio within the threshold even without constraints on renewable energy generation. However, exceeding this threshold requires additional investment in PV and ESS construction, leading to a sudden cost escalation.

Conclusions

Our study introduces a coordinated planning model that encompasses both DERs and BSs, with the primary objective of enhancing communication QoS. Communication QoS, assessed through CR and DTR, serves as the cornerstone of our model. These factors are elegantly captured using a logarithmic function, which takes into account the transmit power of the communication system. Furthermore, we incorporate CR into our model to mitigate bit error rates during communication. Case studies based on in standard and actual distribution network demonstrate the following.

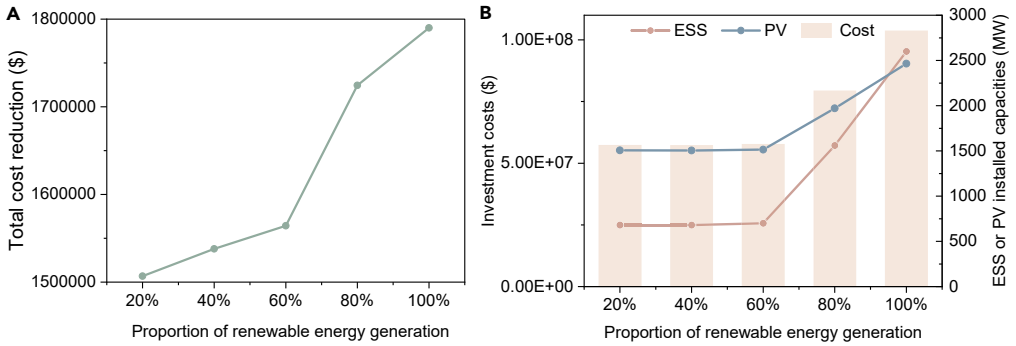

Figure 4. Planning results of communications and power coordination planning (CPCP) in the context of low-carbon transition

(A) The reduction in investment cost of CPCP compared to strategy M1 under various proportion of renewable energy generation.

(B) Changes in energy storage system (ESS) and photovoltaic (PV) capacities, as well as total investment cost under CPCP strategy, across different proportion of renewable energy generation.

(1) At cyber layer, our proposed BS access mechanism optimizes the communication topology between users and BSs. This results in an efficient and tailored communication network where each user accesses the most suitable BS. The outcome is the maximization of total communication capacity within MGs. This has profound implications for communication system planning and operation, as it ensures that resources are efficiently allocated to deliver high-quality communication services.

(2) At physical layer, the coordination planning model, which considers communication quality as a fundamental parameter, plays a pivotal role in ensuring reliable energy sharing among various market members. High-quality communication services enable seamless coordination and efficient sharing of energy resources. This aspect is crucial for both power and communication system operators to guarantee stable and dependable energy distribution.

(3) Coordinated planning not only leads to cost savings but also contributes to the overall sustainability of the infrastructure. Policies that promote joint optimization of communication and power systems can lead to a more economical and environmentally friendly network, aligning with sustainability goals and energy transition objectives.

Our research not only addresses specific planning and optimization challenges but also presents a comprehensive approach with broader implications. It underscores the pivotal role of efficient communication infrastructure in modern power systems. This holistic approach has the potential to revolutionize how we plan and operate both communication and power systems, ultimately leading to more resilient, cost-effective, and reliable networks. For future work, three issues deserve an in-depth study: (1) in-depth analysis of communication latency and related factors; (2) diverse BS channel allocation strategies in coordinated planning; and (3) design of cooperative mechanisms for equitable benefit distribution.

Limitations of the study

Firstly, one limitation of this study is the omission of considering the influence of communication latency and other related factors on the cooperative planning of information-physical systems during the modeling of the communication aspect. Secondly, this study lacks of exploration regarding the heterogeneous BS channel allocation strategies for different users. In practice, users within a communication network often exhibit diverse requirements and characteristics, and their BS channel allocation needs may vary accordingly. Finally, the collaboration between two distinct entities necessitates the design of cooperative mechanisms to incentivize or strengthen the joint cooperation between systems, ultimately achieving a win-win situation for all parties involved. However, this paper solely focuses on exploring different strategies of cooperation, without delving into the design of collaborative mechanisms for equitable benefit distribution. This aspect warrants a separate research endeavor to comprehensively discuss and analyze.

Furthermore, it is important to note that the effectiveness of the theoretical model in real-world applications will show significant variability due to different system boundary conditions, which can mainly be outlined in the following three aspects:

(1) Differences in resource endowment, power grid topology, and user demand characteristics in different regions: This is mainly reflected in the constraints related to the operation of the power system in the model. Generally speaking, the larger the scale of the communication system, and the higher the mismatch between distributed resources and power load, the more significant the effect of cooperative planning will be.

(2) Differences in communication service quality requirements between different regions and users: This is mainly reflected in the QoS-related constraints in the model. In this paper, we only consider the CR and DTR as QoS evaluation indicators. In actual systems, communication service quality requirements may include more dimensions, and communication latency and diverse base station channel allocation strategies will also affect the results of cooperative planning.

Table 3. List of acronyms

Term	Acronym	Term	Acronym
Active distribution network	ADN	Microgrid	MG
Base station	BS	Information and communication technology	ICT
Communication reliability	CR	Orthogonal frequency division multiple access	OFDMA
Distributed energy resource	DER	Ordinary least squares	OLS
Downlink transmission rate	DTR	Photovoltaic	PV
Distribution system operator	DSO	Quality of service	QoS
Energy storage system	ESS	Signal-to-noise ratio	SNR

(3) Different technological preferences in various regions: This is mainly reflected in the constraints related to investment decisions in the model. In actual systems, resource investment will also be affected by local incentive policies, cultural, and social factors, among others, which will likewise have a significant impact on the results of cooperative planning.

Acronyms

The acronyms used in this paper are listed in Table 3.

STAR★METHODS

Detailed methods are provided in the online version of this paper and include the following:

- KEY RESOURCES TABLE
- RESOURCE AVAILABILITY
  - Lead contact
  - Materials availability
  - Data and code availability
- METHOD DETAILS
  - Communication network model
  - Coordinated planning model
  - Solution algorithm
  - Data resources

SUPPLEMENTAL INFORMATION

Supplemental information can be found online at https://doi.org/10.1016/j.isci.2024.109290.

ACKNOWLEDGMENTS

This work was supported by National Key R&D Program of China (No. 2022YFB2405600) and National Natural Science Foundation of China (No. 52207098, 52277092).

AUTHOR CONTRIBUTIONS

Conceptualization, L.C., J.W., and Z.W.; methodology, L.C. and J.W.; investigation, L.C. and Y.Y; writing – original draft, L.C., J.L., and Z.W.; writing – review and editing, L.C. and Z.W.; visualization, L.C.; supervision, Y.Y., G.L., and M.Z.; funding acquisition, J.W and Z.W.

DECLARATION OF INTERESTS

The authors declare no competing interests.

DECLARATION OF GENERATIVE AI AND AI-ASSISTED TECHNOLOGIES IN THE WRITING PROCESS

During the preparation of this work the authors used chatGPT3.5 in order to improve language and readability. After using this tool/service, the authors reviewed and edited the content as needed and take full responsibility for the content of the publication.

Received: October 16, 2023
Revised: February 1, 2024
Accepted: February 16, 2024
Published: February 20, 2024

REFERENCES

1. Wu, Z., Zhou, M., Zhang, Z., Zhao, H., Wang, J., Xu, J., and Li, G. (2022). An incentive profit-sharing mechanism for welfare transfer in balancing market integration. Renew. Sustain. Energy Rev. *168*, 112762.
2. Wang, J., Zhong, H., Yang, Z., Wang, M., Kammen, D.M., Liu, Z., Ma, Z., Xia, Q., and Kang, C. (2020). Exploring the trade-offs between electric heating policy and carbon mitigation in China. Nat. Commun. *11*, 6054.
3. Guan, M., Wu, Z., Cui, Y., Cao, X., Wang, L., Ye, J., and Peng, B. (2019). Efficiency Evaluations Based on Artificial Intelligence for 5G Massive MIMO Communication Systems on High-Altitude Platform Stations. IEEE Trans. Industr. Inform. *16*, 6632–6640.
4. Martins, V.F., and Borges, C.L.T. (2011). Active Distribution Network Integrated Planning Incorporating Distributed Generation and Load Response Uncertainties. IEEE Trans. Power Syst. *26*, 2164–2172.
5. Wu, Z., Zhou, M., Li, G., Zhao, T., Zhang, Y., and Liu, X. (2020). Interaction between balancing market design and market behaviour of wind power producers in China. Renew. Sustain. Energy Rev. *132*, 110060.
6. Kong, P.Y., and Song, Y. (2019). Joint Consideration of Communication Network and Power Grid Topology for Communications in Community Smart Grid. IEEE Trans. Industr. Inform. *16*, 2895–2905.
7. China Center for Information Industry Development. White paper on 5G application development. http://www.xinhuanet.com/tech/2020-12/04/c_1126821689.htm.
8. Ji, B., Wang, Y., Song, K., Li, C., Wen, H., Menon, V.G., and Mumtaz, S. (2021). A Survey of Computational Intelligence for 6G: Key Technologies, Applications and Trends. IEEE Trans. Industr. Inform. *17*, 7145–7154.
9. Zhao, W., Dong, Y., Mo, J., Fang, Z., and Liu, R. (2021). Key technologies and business models of power and communication shared tower. China Power *54*, 171–180.
10. Gutierrez-Rojas, D., Nardelli, P.H.J., Mendes, G., and Popovski, P. (2020). Review of the State of the Art on Adaptive Protection for Microgrids Based on Communications. IEEE Trans. Industr. Inform. *17*, 1539–1552.
11. Memon, S.A., Upadhyay, D.S., and Pate, R.N. (2023). Optimization of solar and battery-based hybrid renewable energy system augmented with bioenergy and hydro energy-based dispatchable source. iScience *26*.
12. Wang, J., Zhong, H., Tang, W., Rajagopal, R., Xia, Q., and Kang, C. (2018). Tri-Level Expansion Planning for Transmission Networks and Distributed Energy Resources Considering Transmission Cost Allocation. IEEE Trans. Sustain. Energy *9*, 1844–1856.
13. Muessel, J., Ruhnau, O., and Madlener, R. (2023). Accurate and Scalable Representation of E-Vehicles in Energy System Models: A Virtual Storage-Based Aggregation Approach (iScience).
14. Li, Y., Wang, Y., Kang, C., Song, J., He, G., and Chen, Q. (2022). Improving distributed PV integration with dynamic thermal rating of power distribution equipment. iScience *25*, 104808.
15. Guo, Y., Xu, J., Duan, L., and Zhang, R. (2014). Joint Energy and Spectrum Cooperation for Cellular Communication Systems. IEEE Trans. Commun. *62*, 3678–3691.
16. Dalmasso, M., Meo, M., and Renga, D. (2016). Radio resource management for improving energy self-sufficiency of green mobile networks. SIGMETRICS Perform. Eval. Rev. *44*, 82–87.
17. Li, D., Saad, W., Guvenc, I., Mehbodniya, A., and Adachi, F. (2015). Decentralized Energy Allocation for Wireless Networks With Renewable Energy Powered Base Stations. IEEE Trans. Commun. *63*, 2126–2142.
18. Mao, Y., Zhang, J., and Letaief, K.B. (2015). A Lyapunov Optimization Approach for Green Cellular Networks With Hybrid Energy Supplies. IEEE J. Sel. Areas Commun. *33*, 2463–2477.
19. Shafi, M., Molisch, A.F., Smith, P.J., Haustein, T., Zhu, P., De Silva, P., Tufvesson, F., Benjebbour, A., and Wunder, G. (2017). 5G: A Tutorial Overview of Standards, Trials, Challenges, Deployment, and Practice. IEEE J. Sel. Areas Commun. *35*, 1201–1221.
20. Xu, L., Guo, Q., Wang, Z., and Sun, H. (2021). Modeling of Time-Delayed Distributed Cyber-Physical Power Systems for Small-Signal Stability Analysis. IEEE Trans. Smart Grid *12*, 3425–3437.
21. Chen, L., Wang, J., Wu, Z., Li, G., Zhou, M., Li, P., and Zhang, Y. (2021). Communication reliability-restricted energy sharing strategy in active distribution networks. Appl. Energy *282*, 116238.
22. Khodr, H.M., Olsina, F.G., Jesus, P.D.O.D., and Yusta, J.M. (2008). Maximum savings approach for location and sizing of capacitors indistribution systems. Elec. Power Syst. Res. *78*, 1192–1203.
23. Wang, J., Zhong, H., Lai, X., Xia, Q., Wang, Y., and Kang, C. (2017). Exploring Key Weather Factors From Analytical Modeling Toward Improved Solar Power Forecasting. IEEE Trans. Smart Grid *10*, 1417–1427.
24. Zhang, T., Wang, J., Zhong, H., Li, G., Ming, Z., and Zhao, D. (2023). Soft open point planning in renewable-dominated distribution grids with building thermal storage. CSEE J Power Energy Syst. *9*, 244–253.
25. Brown, S.H. (2009). Multiple linear regression analysis: A matrix approach with MATLAB. Alabama J. Math. 1–3.
26. (2023). Pecan Street website. https://www.dataport.cloud/.
27. PJM (2023). Day-Ahead Hourly LMPs. http://dataminer2.pjm.com!feed/da_hrl_lmps/definition.
28. Wang, J., Zhong, H., Qin, J., Tang, W., Rajagopal, R., Xia, Q., and Kang, C. (2019). Incentive mechanism for sharing distributed energy resources. J. Mod. Power Syst. Clean Energy *7*, 837–850.
29. Arnold, O., Richter, F., Fettweis, G., and Blume, O. (2010). Load consumption modeling of different base station types in heterogeneous cellular networks. Future Netw. Mobile Summit, 1–8.

STAR★METHODS

KEY RESOURCES TABLE

REAGENT or RESOURCE	SOURCE	IDENTIFIER
Deposited data		
The yearly load and solar power data	Pecan Street website	https://www.dataport.cloud/
The yearly LMP data	PJM	http://dataminer2.pjm.com!feed/da_hrl_lmps/definition.
Macro base station power model parameters	Oliver Arnold	https://ieeexplore.ieee.org/abstract/document/5722444/references#references
New data generated by this study (data used for figures)	This study	Data S1
Software and algorithms		
MATLAB R2021b	MathWorks	https://matlab.mathworks.com/
YALMIP	Johan Löfberg	https://yalmip.github.io/
CPLEX	IBM	https://www.ibm.com/cn-zh/products/ilog-cplex-optimization-studio

RESOURCE AVAILABILITY

Lead contact

Further information and requests for resources should be directed to and will be fulfilled by the lead author, Professor Jianxiao Wang (wang-jx@pku.edu.cn).

Materials availability

This study did not generate new unique materials.

Data and code availability

- This study analyzes existing, publicly available data which are listed in the key resources table. The data generated by our analysis can be found in Data S1.
- This study does not report original code, which is available for academic purposes from the lead contact.
- Any additional information required to reanalyze the data reported in this paper is available from the lead contact upon request.

METHOD DETAILS

Communication network model

The communication network is to maintain the QoS in energy sharing among different MGs. Specifically, we first introduce the indicators of QoS, i.e., the CR and DTR. Then, the relationship between the signal-to-noise ratio (SNR) and the BS transmit power will be discussed. Finally, the base station access mechanism as well as the interaction between the power consumption and the QoS of communication are discussed.

The QoS model we use in this study is improved from our previous work.[21] Each EMC is able to communicate with the DSO and receives control commands with the support of a communication network. To evaluate the quality of each communication, the CR and DTR are selected as indicators. The CR between the base station and the EMC in a dedicated power wireless network satisfies a specific value α., which has been specifically discussed in 21. The users' information transmission rates are greater than a given threshold β (Mbps). The thresholds for CR and DTR are not guaranteed without a dedicated power wireless network. The CR and DTR of each MG are calculated as follows:

$$\delta_{n-i} = \left[1 - Q\left(\sqrt{2SNR_{n-i}\frac{B^N}{R}}\right)\right]^l \geq \alpha \quad \text{(Equation 1)}$$

$$c_{n-i} = \frac{B}{K}\log_2(1 + SNR_{n-i}) \geq \beta \quad \text{(Equation 2)}$$

Here, in the CR formula, δ_{n-i} denote the CR in the communication between BS n and EMC i, $Q(\cdot)$ denote the integral tail function, which obeys standard Gaussian distribution, B^N and R denote the noise bandwidth and data transmission speed in communication, SNR_{n-i} denote

the SNR, and l is the bit length of a packet. In the DTR formula, c_{n-i} is the downlink transmission rate of EMC i, and B is the operating spectrum bandwidth of the BS, and K is the number of allocated orthogonal channels.

According to the properties of the integral tail function and the logarithmic function, the CR and DTR will improve with an increasing SNR, as shown in Figure S1. In this paper, the widely used scheme of equal bandwidth sharing among the EMCs is adopted. The bandwidth assigned to each EMC is B/K. SNR modelling will be introduced in detail in the subsequent text.

The SNR is defined as the ratio of the effective signal strength to the noise signal strength in communication, such as the interference power from other base stations as well as thermal noise interference, and can be presented as follows:

$$SNR_{n-i} = \frac{T_n^E \cdot \left(10^{\frac{PL(d_{n-i})}{10}}\right)^{-1}}{\sum_{m \neq n} T_m^E \cdot \left(10^{\frac{PL(d_{m-i})}{10}}\right)^{-1} + N_0} \quad \text{(Equation 3)}$$

where T_n^E is the transmit power of BS n, T_m^E is the interference power imposed on EMC i by the other BSs, PL is the dB form of the path-loss model, d_{n-i} is the distance between EMC i and BS n, and N_0 is the thermal noise. Therefore, one can improve the transmit power of base stations for SNR enhancement to guarantee that the CR and DTR requirements are met. It should also be noted that, for a certain base station, the increase of the corresponding transmit power can lead to the increase of the interference noise for the other BSs, as shown in Figure S2.

That is to say, it is desirable to determine the appropriate transmit power for geographically distributed base stations to make a tradeoff between communication reliability and related incurred cost. Furthermore, the relationship between the energy consumption of a certain base station and the corresponding transmit power can be expressed as follows:

$$P_n^B = e \cdot n_n^{acc} T_n^E + f \quad \text{(Equation 4)}$$

$$T_{n\min}^E \leq T_n^E \leq T_{n\max}^E \quad \text{(Equation 5)}$$

Where P_n^B is the energy consumption of base stations; T_n^E denoets the transmit power; e and f denote the related coefficients between energy consumption and the corresponding transmit power. $T_{n\min}^E$ and $T_{n\max}^E$ depict the limits of transmit power of base stations.

Because of the use of orthogonal frequency division multiple access (OFDMA), there is no interference between subcarriers of the same BS. The power consumption of BS n increases linearly with its total transmit power, including all subcarriers. Intuitively, the power load of a BS has a linear relationship with its communication load.

In this paper, the BS access scheme is modelled via OFDMA. Note that the use of OFDMA is convenient for performance evaluation. Through this access scheme, the number of subcarriers available to users from each BS is determined. The BSs assign an orthogonal channel to each EMC for downlink transmission.

To describe the access mechanism between the EMCs and the BSs, we introduce an $N_{bs} \times N_{mg}$ connection matrix A, where N_{mg} is the EMCs number and N_{bs} is the number of power towers which is also the number of candidate locations for base stations. It is not necessary for all power towers to be selected as communication power sharing towers. The elements in A satisfy the following constraints:

$$\sum_{n=1}^{N_{bs}} a_{n-i}^A = 1 \quad \text{(Equation 6)}$$

$$\sum_{i=1}^{N_{mg}} a_{n-i}^A = n_n^A \quad \text{(Equation 7)}$$

where a_{n-i}^A is a binary variable, with $a_{n-i}^A = 1$ denoting that EMC i accesses BS n, and n_n^A is the number of EMCs accessing BS n. Constraint (6) means that each EMC can access only one BS. Constraint (7) means that the number of EMCs accessing BS n is equal to the total state variables of the nth column of the matrix A. The capacity of each BS is D_{cap}. Based on the equal-bandwidth-sharing scheme, the constraint on the capacity allocated to each MG, c_{n-i}, is formulated as follows:

$$n_n^A c_{n-i} \leq D_{cap} \quad \text{(Equation 8)}$$

The sum of the downlink transmission rates of all EMCs connected to BS n is equal to the BS communication load, which is less than the BS's capacity. All constructed BSs are intended to meet high traffic requirements. Let the traffic demand (Mbps) in the distribution network area be denoted by D_{total}. Then, the number of BSs to be constructed is restricted as follows:

$$n^{BS} D_{cap} \geq D_{total} \quad \text{(Equation 9)}$$

where n^{BS} is the number of BSs to be constructed in the distribution network area.

As shown in Figure S3 each user accesses a base station, and the BS then allocates a channel to each new user when there is remaining channel capacity. If all of the channel capacity of a BS is occupied, a user cannot access this BS and must instead access another BS that is farther away.

Coordinated planning model

In this section, the coordinated planning model of DERs and BSs is proposed. The objective function aims to minimize the overall cost for distribution system operation consisting of multiple EMCs, including the investment cost for both the energy and communication system:

$$\min C = C_{Inv} + wC_{Ope} \quad \text{(Equation 10)}$$

with

$$w = 365\frac{\mu_{Ope}}{(1+a)^y} \quad \text{(Equation 11)}$$

$$C_{Inv} = \kappa_{PV}\sum_{i\in G_{PV}} c_{PV}n_i^{PV} + \kappa_{ESS}\sum_{i\in G_{ESS}} c_{ESS}n_i^{ESS} + \kappa_{BS}\sum_{i\in G_{BS}} c_{BS}u_i^{BS} \quad \text{(Equation 12)}$$

$$C_{Ope} = \sum_i\sum_t\sum_s \gamma_s\left[\lambda_t^R\left(\sum_{j\in\varphi_i} P_{ijst} - P_{ist}^B\right) - U_i\left(P_{ist}^L\right) + \lambda_t^B P_{ist}^B\right] \quad \text{(Equation 13)}$$

$$\kappa = \frac{a(1+a)^y}{(1+a)^y - 1} \quad \text{(Equation 14)}$$

where C_{Inv} represents the investment cost for DERs and BSs, C_{Ope} is the annual operational cost, w is the equivalent factor of net present value, μ_{Ope} scales the relevant cost into one year. a and y denote the annual interest rate and the expected number of the service year, respectively. G, κ and c represent the set of candidate investment nodes, the equivalent coefficients for annual investment and the unit investment prices, respectively, for PV panels, ESSs and BSs. n_i^{PV} and n_i^{ESS} are the numbers of PV panels and ESSs, respectively, installed at node i: n_i^{BS} is a binary variable indicating whether to establish a BS at node i; and $U_i(\cdot)$ denote the corresponding utility function of EMC i. The operating cost includes the power purchase cost minus the electricity utility. It should be noted that, we predefined the retail rates for all market members, which is considered to be constant in the proposed coordination process.

The constraints of the coordinated planning model are presented as follows:

(1) Power balance and nodal angle/voltage constraints

$$P_{ist}^L - n_{i,PV}P_{ist}^{PV} + n_{i,ESS}\left(P_{istc}^{ESS} - P_{istd}^{ESS}\right) + u_{i,BS}P_{ist}^B + \sum_{j\in\varphi_i} P_{ijst} = 0 \quad \text{(Equation 15)}$$

$$Q_{ist}^L + n_{i,ESS}Q_{ist}^{ESS} + \sum_{j\in\varphi_i} Q_{ijst} = 0 \quad \text{(Equation 16)}$$

$$V_{\min} \le V_{ist} \le V_{\max} \quad \text{(Equation 17)}$$

$$\theta_{\min} \le \theta_{ist} \le \theta_{\max} \quad \text{(Equation 18)}$$

where P_{istc}^{ESS} and P_{istd}^{ESS} denote the charging and discharging power of the storage system, respectively; P_{ist}^{PV} denote the available generation power of rooftop solar system; Q_{ist}^{ESS} and Q_{ist}^{L} denote the reactive power of energy storage system and residual load, respectively. $V_{\min}$ and $V_{\max}$ depict the boundaries for the amplitude of the voltage; $\theta_{\min}$ and $\theta_{\max}$ depict the boundaries of the phase angle of the voltage.

(2) DER-related constraints

The constraints of solar power and ESS system are shown in Equations 19, 20, 21, 22, 23, and 24, respectively.

$$0 \le P_{ist}^{PV} \le P_{ist}^{FPV} \quad \text{(Equation 19)}$$

$$0 \le P_{istc}^{ESS} \le P_{ic\ \max}^{ESS} \quad \text{(Equation 20)}$$

$$0 \leq P_{istd}^{ESS} \leq P_{id\ \max}^{ESS} \quad \text{(Equation 21)}$$

$$E_{ist}^{ESS} = E_{ist-1}^{ESS} + \eta_i^{ESS} P_{istc}^{ESS} - P_{istd}^{ESS} / \eta_i^{ESS} \quad \text{(Equation 22)}$$

$$E_{i\ \min}^{ESS} \leq E_{ist}^{ESS} \leq E_{i\max}^{ESS} \quad \text{(Equation 23)}$$

$$E_{is0}^{ESS} = E_{isT}^{ESS} \quad \text{(Equation 24)}$$

where P_{ist}^{FPV} denotes the available solar power; $P_{ic\ \max}^{ESS}$ and $P_{id\ \max}^{ESS}$ are the maximum amounts of charged and discharged power, respectively, for an energy storage system (ESS); η_i^{ESS} is the efficiency of the energy storage; E_{ist}^{ESS}, $E_{i\ \min}^{ESS}$ and $E_{i\ \max}^{ESS}$ are the capacity limits of the energy storage; E_{is0}^{ESS} and E_{isT}^{ESS} are stored energy levels in of the energy storage in the first and the last time slot.

(3) Power flow constraints

The power injection and the capacity constraint of the transmission line can be expressed as follows:

$$\left(P_{ijst}\right)^2 + \left(Q_{ijst}\right)^2 \leq \left(S_{ijst}\right)^2 \quad \text{(Equation 25)}$$

$$P_{ijst} = g_{ij}\left(V_{ist}^2 - V_{ist}V_{jst}\cos\theta_{ijst}\right) - b_{ij}V_{ist}V_{jst}\sin\theta_{ijst} \quad \text{(Equation 26)}$$

$$Q_{ijst} = -b_{ij}\left(V_{ist}^2 - V_{ist}V_{jst}\cos\theta_{ijst}\right) - g_{ij}V_{ist}V_{jst}\sin\theta_{ijst} \quad \text{(Equation 27)}$$

When the network losses are ignored, the linear power flow equations are as follows:[24]

$$P_{ijst} = g_{ij}\frac{\left(V_{ist}^2 - V_{jst}^2\right)}{2} - b_{ij}\left(\theta_{ist} - \theta_{jst}\right) \quad \text{(Equation 28)}$$

$$Q_{ijst} = -b_{ij}\frac{\left(V_{ist}^2 - V_{jst}^2\right)}{2} - g_{ij}\left(\theta_{ist} - \theta_{jst}\right) \quad \text{(Equation 29)}$$

where g_{ij} and b_{ij} denote the susceptance and conductance of the distribution network, respectively; V_{ist} and θ_{ist} denote the voltage amplitude and phase angle, respectively. A relaxation approach for non-convex constraints (25) is applied to linearize the original primal problem, as shown in Figure S4. The area of a circle can be approximated by the area of its inscribed polygon consist of a set of lines.

Let the number of segments of the boundary circle be denoted by M, i.e., $\psi = \frac{2k\pi}{M}$, $k \in 1, 2...M$. Then, constraint (25) can be linearized in a piecewise form as follows:

$$P_{ijst}\cos\psi + Q_{ijst}\sin\psi \leq S_{ijst}\cos\frac{\psi}{2} \quad \text{(Equation 30)}$$

(4) QoS-related constraints

As indicated above, constraints (1)-(5) represent CR and DTR requirements, and constraints (6)-(9) represent base station capacities requirement. In the M1 and CPCP strategies, these two requirements should be satisfied at the same time. However, in the M2 strategy, only constraints (6)-(9) should be satisfied. Besides, it is worth mentioning that the objective functions (1)-(3) are also nonlinear constraints. Due to the high computational burden incurred by nonlinear problem solvers, a linearization method is introduced in next section.

Solution algorithm

In this section, we propose a transformation method for constraints (1)-(3) based on a multiple linear regression model to obtain equivalent constraints in linear form.

(1) Transformation

Based on the derivation of Equations 1 and 2, we propose the following theorem.

Theorem 1: The constraints $\delta_{n-i} \geq \alpha$ and $c_{n-i} \geq \beta$ can be considered equivalent to $SNR_{n-i} \geq \tau_1$ and $SNR_{n-i} \geq \tau_2$.

Proof 1: Equations 1 and 2 are functions of the SNR, and their partial derivatives are as follows:

$$\frac{\partial \delta}{\partial SNR} = I \cdot \left[1 - Q\left(\sqrt{2SNR\frac{B^N}{R}}\right)\right]^{I-1} \cdot \frac{1}{\sqrt{2\pi}} \exp\left(-SNR\frac{B^N}{R}\right) \quad \text{(Equation 31)}$$

$$\frac{\partial c}{\partial SNR} = \frac{B}{\ln 2 \cdot SNR \cdot K} \quad \text{(Equation 32)}$$

Since the SNR is always greater than 0, we can draw the following conclusions:

$$\frac{\partial \delta}{\partial SNR} \geq 0 \text{ and } \frac{\partial c}{\partial SNR} \geq 0 \quad \text{(Equation 33)}$$

Therefore, δ and c increase monotonically with respect to the *SNR*. Thus, Theorem 1 can be proven:

$$\delta_{n-i} \geq a \Longleftrightarrow SNR \geq \arg \delta_{n-i}|_a \quad \text{(Equation 34)}$$

$$c_{n-i} \geq \beta \Longleftrightarrow SNR \geq \arg c_{n-i}|_\beta \quad \text{(Equation 35)}$$

Based on Theorem 1, the CR and DTR requirements can be considered equivalent to a basic guarantee concerning the SNR.

(2) Multiple linear regression Estimation

The *SNR* is still nonlinear in Equation 3. According to the principle of least squares linear fitting in a multidimensional space, the regression equation for $SNR_{n-i}(T_n^E)$ can be reformulated as follows:

$$SNR_{n-i} = T^E C + \varepsilon \quad \text{(Equation 36)}$$

where SNR_{n-i} is a random vector consisting of the k × 1-dimensional observations; T^E is a matrix determined by k × (n+1) predictors; C denotes a vector of (n+1) × 1 unknown parameters, with $c_0, c_1 \ldots, c_n$ being regression coefficients, which represent the unrelated contributions of each independent variable W_{jn}^E toward predicting the dependent variable $SNR_{n-i,j}$; and ε is a k × 1 vector of errors between the predicted and true values.

Theorem 2: When $E(\varepsilon) = 0$, the regression coefficients $\widehat{C}$ calculated using the ordinary least squares (OLS) method are an unbiased estimate of C.

Proof 2: The regression coefficients based on OLS method can be obtained by minimizing the total squared errors:

$$\left(T^E\right)^T T^E \widehat{C} = \left(T^E\right)^T SNR_{n-i} \quad \text{(Equation 37)}$$

where $\widehat{c_n}$ is the OLS estimator and its matrix notation is $\widehat{C}$.[25] Noted that the variables $T_1^E, T_2^E, \ldots, T_n^E$ are linearly independent, that is to say, the inverse of $(T^E)^T T^E$, denoted as ξ, will exist.

Then, by multiplying the inverse of $(T^E)^T T^E$, i.e., ξ, the Equation 29 can be transformed to the following form:

$$\widehat{C} = \xi \cdot \left(T^E\right)^T SNR_{n-i} \quad \text{(Equation 38)}$$

We can use the definition of SNR_{n-i} to rewrite the OLS estimator as follows:

$$\widehat{C} = \xi \cdot \left(T^E\right)^T \left(T^E C + \varepsilon\right) = C + \xi \cdot \left(T^E\right)^T \varepsilon \quad \text{(Equation 39)}$$

Therefore, the expectation of $\widehat{C}$ is:

$$E(\widehat{C}) = C + \xi \cdot \left(T^E\right)^T \cdot E(\varepsilon) = C + \xi \cdot \left(T^E\right)^T \cdot 0 = C \quad \text{(Equation 40)}$$

Thus, when $E(\varepsilon) = 0$, the expectation of the parameter estimator $\widehat{SNR}_{n-i} = T^E \widehat{C}$ obtained via the OLS method approximates its true value SNR_{n-i}. Furthermore, the constraints $SNR_{n-i} \geq \tau_1$ are equivalent to $T^E \widehat{C} \geq \tau_1$.

Data resources

We first conduct the case studies in the IEEE 33-bus system. Each node represents an MG with adjustable loads and is also a candidate point for the construction of PV panels, ESSs and BSs. The discount rate a was set to 5%, and the service lives of the PV panels, ESSs and BSs were set to 10, 7 and 5 years, respectively. Therefore, the annual investment equivalent coefficients for PV panels, ESSs and BSs were 0.1295, 0.1728, and 0.231, respectively. Accordingly, μ_{Ope} and w are set to 1+0.5*a* and 229.68. The investment costs for an ESS with a 20 MWh capacity and an equivalent 5G communication BS for an MG were taken to be \$ 1×10^6 and \$ 6 × 10^6, respectively, and the investment cost for a 1-MW

solar panel was taken to be $ 2.4 × 10^5. The yearly load and solar power data are from Pecan Street website.[26] The yearly LMP data are from PJM.[27]

The relevant parameters of energy storage system are shown in Table S1.[28] We chose to model a macroscale base station and the parameter of the corresponding path-loss model is shown in Table S2, and the other related parameters of the communication network are also listed in the same table.[29]